PERGAMON

International Journal of Heat and Mass Transfer 45 (2002) 331–341

International Journal of HEAT and MASS TRANSFER

www.elsevier.com/locate/ijhmt

Conjugate forced convection–conduction heat transfer analysis of a heat generating vertical cylinder

G. Jilani *, S. Jayaraj, M. Adeel Ahmad

Department of Mechanical Engineering, Regional Engineering College, Calicut 673601, India

Received 20 July 1999; received in revised form 10 April 2001

Abstract

Conjugate heat transfer by forced convection over a vertical cylinder without heat generation has been a subject of many investigations in the recent past. In the present work, the radial heat conduction along with heat generation in a vertical cylinder is considered for analysis. The steady two-dimensional conduction equation for the heat generating cylinder and steady two-dimensional laminar boundary layer equations for the flowing fluid are solved simultaneously using a finite-difference scheme. Results are presented for a wide range of conduction–convection, heat generating parameters and length to diameter ratio for a specific fluid having Prandtl number 0.005. It is found that the radial temperature distribution in the boundary layer as well as the cylinder are remarkably significant especially with the inclusion of internal heat generation in the cylinder.

1. Introduction

Conjugate heat transfer refers to the heat transfer processes involving an interaction of conduction in a solid body and convection in the fluid surrounding it. Thus the analysis of this type of heat transfer processes necessitates the coupling of the conduction in the solid and the convection in the fluid present. The conditions of continuity in temperature and heat flux has to be fulfilled at the fluid–solid interface. Conjugate heat transfer occurs in many important engineering devices. A common example is a heat exchanger in which the conduction in solid tube wall is greatly influenced by the convection in fluid flowing over it. Another example of practical importance of conjugate heat transfer is found in fins. The conduction within the fin and convection in the fluid surrounding it must be simultaneously analysed to obtain vital design information.

The conjugate heat transfer finds yet another very important application in the fuel element of a nuclear reactor. During normal operation of a nuclear reactor, the internal heat generated in the fuel element must be dissipated and carried away by a stream of coolant passing over it. If the heat generated is not removed fast enough by the coolant, the fuel element may heat up so much that eventually a part of the core may melt. Hence the problem is the one of heat removal without excessively high temperature inside fuel elements or on their surfaces. A knowledge of the temperature distribution in the fuel element is needed in order to predict its performance, in particular the highest fuel element temperature and the rate of heat removal. This necessitates a detailed conjugate heat transfer analysis of the heat generating fuel element washed by forced flow. Conventional heat transfer analyses pertaining to applications of similar nature are based on the assumptions of a uniform surface temperature or the surface heat flux, which actually varies over the solid surface.

The conjugate heat transfer problem of laminar forced convection along a flat plate of finite thickness has been analysed by Luikov et al. [1]. They solved the problem by means of the generalized Fourier sine transformation and a series expansion in terms of the Fourier variable. Luikov [2] has given an approximate solution of the above conjugate heat transfer problem by means of the generalized Fourier sine transformation and a series expansion in terms of the Fourier variable. Luikov [2] has given an approximate solution of the above conjugate heat transfer problem assuming a linear

* Corresponding author. Tel.: +91-495-286-403; fax: +91-495-287-250.

E-mail address: jilani@crec.ker.nic.in (G. Jilani).

0017-9310/02/$ - see front matter
PII: S0017-9310(01)00140-5

Nomenclature

Lower case symbols given in parentheses are the dimensional counterparts of the dimensionless equivalents written on the same line

Fi	conduction–convection parameter $((k_f/k_s)(r_0/L)Re^{1/2})$
h	local heat transfer coefficient
h_N	non-dimensional local heat transfer coefficient $(h(L/k_f)Re^{-1/2})$
k	thermal conductivity
L	characteristic length of the cylinder
n	number of grids in the R-direction, in the flow field
P	parameter representing length to diameter ratio of the cylinder $(4L^2/D^2)$
Pr	Prandtl number
q'''	internal heat generation per unit volume in the cylinder
Q	non-dimensional internal heat generation parameter $(q'''r_0^2/(t_0 - t_\infty)k_s)$
R (r)	radial co-ordinate normal to the cylinder surface
R_0 (r_0)	radius of the cylinder
R_1	non-dimensional radial coordinate used in the two-dimensional heat conduction equation
Re	Reynolds number $(U_\infty L/v)$
R_s	non-dimensional distance from the cylinder surface $(R - R_0)$
T (t)	temperature
t_0	maximum allowable cylinder temperature
U (u)	velocity component in X-direction
V (v)	velocity component in R-direction
X (x)	stream-wise co-ordinate along the cylinder length

Greek symbols

α	thermal diffusivity of the fluid
β	ratio of grid sizes $(\Delta R_1/\Delta X)$
v	kinematic viscosity of the fluid
σ	ratio of smaller to larger grid size in R-direction

Subscripts

f	fluid
j	location in X-direction
k	location in R-direction
s	solid
∞	free stream

Superscript

$*$	value from previous iteration

temperature distribution in the flat plate and suggested certain design formulae for the calculation of local Nusselt number. Karvinen [3] presented an approximate method for solving the conjugated heat transfer from a flat plate in forced flows in the presence of uniform internal heat generation. The results have been compared with available experimental data.

Sparrow and Chyu [4] carried out a conjugate heat transfer analysis for a vertical plate fin washed by laminar forced convection boundary layer flow. They assumed the heat conduction in the fin to be one-dimensional. The results obtained from the numerical solutions have been compared with those from the conventional methods. Huang and Chen [5] have studied a vertical thin circular pin fin in forced convective flow. They have considered one-dimensional heat conduction in the longitudinal direction. The conservation equations for the laminar boundary layer and the energy equation for the fin have been solved simultaneously by an efficient implicit difference scheme. The results are presented for a range of values of conjugated convection–conduction parameter and the transverse curvature parameter. Velusamy and Garg [6] have obtained the heat transfer characteristics for a vertical cylindrical fin washed by a combined forced and free convective flow. They have also followed a simultaneous solution to conduction problem for the fin and laminar boundary layer equations for the flowing fluid. The effect of various parameters such as the conduction-convection parameter, the buoyancy influence parameter and the dimensionless radius on the fin temperature distribution and the heat flux rate has been analysed numerically by treating one-dimensional heat conduction in the fin. The results obtained for $Pr = 0.7$ have been compared with those of the conventional mode. It is observed that the conventional model overpredicts the fin effectiveness at small values of conduction–convection parameter. It is also pointed out by Velusamy and Garg [6] that for forced flow at any value of conduction–convection parameter, local heat transfer coefficient decreases monotonically in the flow direction as the boundary layer grows.

An accurate solution of the coupled forced convection–conduction problem for a horizontal flat plate has been given by Pozzi and Lupo [7]. They analyzed the entire thermo-fluid – dynamic field by means of two expansions in terms of coupling parameter. Yu et al. [8] proposed a very effective solution method to solve the conjugate problems of forced convection in incompressible laminar boundary layer flow with constant properties and heat conduction in a solid wall. For flows passing a flat plate and a wedge, very accurate finite

difference solutions of interface temperature and heat transfer rates are presented over the entire thermo-fluid-dynamic field for any Prandtl number between 0.0001 and infinity. Comprehensive correlation equations of the local Nusselt numbers are obtained, which are in good agreement with numerical data. Exact solutions are also presented for the conjugate problems of the stagnation flow and a rotating cone or disk.

Two-dimensional heat conduction in the solid for the analysis of forced convective conjugate heat transfer problem was not considered in any of the above investigations. In addition, most of the analyses available in literature are based on the assumption of no heat generation in the solid. This simplification may hold good for certain engineering applications but definitely not valid for many important applications such as the fuel element of a nuclear reactor. In the latter case, radial heat conduction also needs to be taken into account in addition to the axial heat conduction. Most of the analyses of forced convective conjugate heat transfer reported in the literature are limited to either horizontal or vertical flat plate. Only Huang and Chen [5] and Velusamy and Garg [6] have studied the conjugate heat transfer from a vertical cylindrical fin. They too have not included radial heat conduction into their analysis.

The present work deals with the analysis of the conjugate heat transfer in a heat generating vertical cylinder washed by a laminar forced convection boundary layer flow. The objective of this investigation is to study the effect of various parameters on temperature profiles and important heat transfer characteristics by including radial heat conduction in the analysis. Accordingly, the governing partial differential equations for the cylinder and flowing fluid are solved simultaneously by satisfying the continuity of the heat flux and the temperature at the interface. While the boundary layer equations are solved by a fully implicit finite difference marching technique, the two-dimensional heat conduction equation is solved by the line by line method.

2. Mathematical formulation

A heat generating vertical cylinder washed by an upwardly flowing stream of a fluid is considered as shown in Fig. 1. The lower end of the cylinder is assumed to be maintained at the free stream temperature while the upper end is insulated. The heat transfer mechanism involves the following two phenomena:

(a) conduction inside the cylinder, and
(b) convection from the cylinder surface to the flowing fluid.

The velocity and temperature distributions in the flow field are governed by the boundary layer equations, while the temperature distribution inside the cylinder is

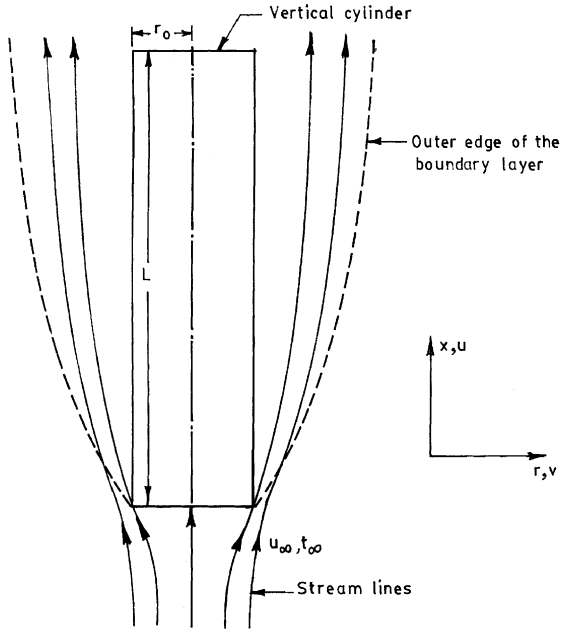

Fig. 1. Flow past a vertical cylinder.

governed by the two-dimensional heat conduction equation. The following important assumptions are made in the present analysis:

(i) the thermophysical properties variation of the fluid are negligible,
(ii) the flow is steady, laminar, two-dimensional and incompressible,
(iii) the heat generation is uniform throughout the cylinder,
(iv) the thermal conductivity of the cylinder material does not change with temperature, and
(v) the cylinder material is homogeneous and isotropic.

Symmetry about the cylinder centerline enables only half of the cylinder needs to be taken as the domain for obtaining two-dimensional temperature distribution inside the cylinder. Also the temperature gradient along the cylinder centerline is zero. The boundary condition at the cylinder surface (i.e., at the interface between the solid and the fluid) is governed by the requirement that the heat flux and temperature be continuous. Since the fluid velocity at the surface of the cylinder is zero due to the no slip condition, the heat transfer from the surface to the fluid in its immediate vicinity is predominantly by conduction and can therefore be given by Fourier's law of heat conduction.

The dimensionless form of the boundary layer equations governing the flow over the vertical cylinder is given by

$$\text{Continuity}: \frac{\partial}{\partial X}(RU) + \frac{\partial}{\partial R}(RV) = 0. \quad (1)$$

$$\text{Momentum}: U\frac{\partial U}{\partial X}+V\frac{\partial U}{\partial R}=\frac{1}{R}\frac{\partial U}{\partial R}+\frac{\partial^2 U}{\partial R^2}. \tag{2}$$

$$\text{Energy}: U\frac{\partial T}{\partial X}+V\frac{\partial T}{\partial R}=\frac{1}{Pr}\frac{1}{R}\frac{\partial T}{\partial R}+\frac{1}{Pr}\frac{\partial^2 T}{\partial R^2}. \tag{3}$$

The non-dimensional form of the boundary conditions for solving these equations will be

$$\begin{aligned} &U(X,R_0)=0, \quad V(X,R_0)=0, \quad T(X,R_0)=T_s(X),\\ &U(X,\infty)=1, \quad T(X,\infty)=0, \quad U(0,R)=1,\\ &T(0,R)=0. \end{aligned} \tag{4}$$

The dimensional form of two-dimensional heat conduction equation in the cylinder with uniform internal heat generation is

$$\frac{\partial^2 T}{\partial X^2}+P\frac{\partial^2 T}{\partial R_1^2}+P\frac{1}{R_1}\frac{\partial T}{\partial R_1}+PQ=0. \tag{5}$$

The non-dimensional form of the boundary conditions for solving the heat conduction equation are

$$\begin{aligned} &T(0,R)=0, \quad \frac{\partial T}{\partial X}(1,R)=0, \quad \frac{\partial T}{\partial R_1}(X,0)=0,\\ &\frac{\partial T}{\partial R_1}(X,1)=Fi\frac{\partial T}{\partial R}(X,R_0),\\ &T_s(X,1)=T_f(X,R_0). \end{aligned} \tag{6}$$

The following non-dimensional parameters were used in the above equations (Eqs. (1)–(6)).

$$\begin{aligned} &X=x/L, \quad R=(r/L)Re^{1/2}, \quad R_0=(r_0/L)Re^{1/2},\\ &R_1=r/r_0, \quad U=u/u_\infty, \quad V=(v/u_\infty)Re^{1/2},\\ &T=(t-t_\infty)/(t_0-t_\infty), \quad Re=u_0L/v, \quad Pr=v/\alpha,\\ &P=4L^2/D^2, \quad Q=q'''r_0^2/(t_0-t_\infty)k_s,\\ &Fi=(k_f/k_s)(r_0/L)Re^{1/2}. \end{aligned} \tag{7}$$

Analytical solution of the governing equations pertaining to the conjugate heat transfer problem (Eqs. (1)–(6)) is not easy owing to the presence of non-linear terms in the boundary layer equations. Therefore, these equations are solved using a finite difference technique. The procedure starts with the solution of the boundary layer equations (Eqs. (1)–(3)) subject to an assumed surface temperature distribution. This results in a knowledge of the temperature in the flow field. Eq. (5) is solved subject to the conjugate boundary conditions (Eq. (6)) using the updated temperature distribution in the flow field. The resulting improved surface temperature distribution is again used to solve the boundary layer equations. The process is repeated until convergence of the cylinder surface temperature distribution is obtained. The boundary layer equations are parabolic in the X-direction and can be solved easily by a marching technique. As the energy equation is decoupled from the continuity and momentum equations, it can be solved once U and V values are known. The two-dimensional heat conduction equation is elliptic in nature and is solved using line by line method.

3. Finite difference solution

In order to represent the dimensionless form of the governing partial differential equations into finite difference form, a two-dimensional rectangular mesh is superimposed on the computational domain. Indices (j,k) are used to indicate position in the (X,R) directions, respectively. The choice of the coordinates is such that (0,0) represents the leading edge both in terms of the indices and the spatial coordinates. A small change by ΔX and ΔR in the X and R directions respectively, increases j and k by 1, the cylinder surface is represented by $k=0$ and the edge of the boundary layer by $k=n+1$.

3.1. Discretization

The boundary layer equations are discretized in such a way that the solution can be carried out by a marching procedure in the X-direction. A highly implicit difference representation is preferred for the Eqs. (2) and (3). Eq. (1) is solved in an explicit stepwise manner. Forward differencing in the marching X-direction and central differencing in the R-direction are employed in Eqs. (2) and (3), whereas only forward differencing is employed in Eq. (1). The finite difference form of the equations selected is given below [9]:

Continuity equation:

$$\frac{R_{k+1}U_{j+1,k+1}-R_{k+1}U_{j,k+1}}{\Delta X}+\frac{R_{k+1}V_{j+1,k+1}-R_kV_{j+1,k}}{\Delta R}=0. \tag{8}$$

Momentum equation:

$$\begin{aligned} &U_{j+1,k}\left[\frac{U_{j+1,k}-U_{j,k}}{\Delta X}\right]+V_{j+1,k}\left[\frac{U_{j+1,k+1}-U_{j+1,k-1}}{2\Delta R}\right]\\ &=\frac{U_{j+1,k+1}-U_{j+1,k-1}}{2R_k\Delta R}+\frac{U_{j+1,k-1}-2U_{j+1,k}+U_{j+1,k+1}}{(\Delta R)^2}. \end{aligned} \tag{9}$$

Energy equation:

$$\begin{aligned} &U_{j+1,k}\left[\frac{T_{j+1,k}-T_{j,k}}{\Delta X}\right]+V_{j+1,k}\left[\frac{T_{j+1,k+1}-T_{j+1,k-1}}{2\Delta R}\right]\\ &=\frac{T_{j+1,k+1}-T_{j+1,k-1}}{2PrR_k\Delta R}+\frac{T_{j+1,k-1}-2T_{j+1,k}+T_{j+1,k+1}}{Pr(\Delta R)^2}. \end{aligned} \tag{10}$$

The above discretization is second order accurate in R for U and T. While obtaining the solution by the

Thomas algorithm, the sufficient conditions to be satisfied by the tridiagonal coefficient matrix elements (Roache [10]) are fulfilled by the discretized Eqs. (9) and (10).

Central differencing is employed in both X and R directions while discretizing the heat conduction equations as given below

$$\frac{T_{j-1,k}-2T_{j,k}+T_{j+1,k}}{(\Delta X)^2}+P\frac{\left[T_{j,k-1}-2T_{j,k}+T_{j,k+1}\right]}{(\Delta R_1)^2}+P\frac{\left[T_{j,k+1}-T_{j,k-1}\right]}{2R_{1k}(\Delta R_1)}+PQ=0. \tag{11}$$

Using L'Hospital's rule the governing equation at the cylinder centerline is written as

$$\frac{T_{j-1,k}-2T_{j,k}+T_{j+1,k}}{(\Delta X)^2}+2P\left[\frac{T_{j,k-1}-2T_{j,k}+T_{j,,k+1}}{(\Delta R_1)^2}\right]+PQ=0. \tag{12}$$

The above discretizations are second order accurate in both the radial and axial directions.

For the boundary condition at the solid–fluid interface backward differencing is employed for the temperature gradient on the solid side, while a three-point polynomial fitting is used to represent the temperature gradient on the fluid side. The discretized form of this equation is given below:

$$\frac{T_{j,k}-T_{j,k-1}}{\Delta R_1}=Fi\left[\frac{-3T_{j,k}+4T_{j,k+1}-T_{j,k+2}}{2(\Delta R)}\right]. \tag{13}$$

3.2. Solution procedure

Equations (8)–(13) are rewritten in a form which readily adaptable for solution. The computation of the values of U, V and T in the flow field is carried out by a marching procedure, starting from the leading edge ($X=0$). The discretized momentum equation (Eq. (9)) written for $k=1(1)n$ leads to a set of n nonlinear equations for n unknown values of U at the X-location $(j+1)$. This set is reduced to a linear set by replacing the coefficients $U_{j+1,k}$ and $V_{j+1,k}$ in the non-linear terms of Eq. (9) by their known values at the previous iteration. The linearized tridiagonal set is solved iteratively using the discretized continuity equation (Eq. (8)) to update V at the location $(j+1)$ till an accuracy of 0.01 is achieved. Once the values of U and V have been obtained at location $(j+1)$, the discretized energy equation (Eq. (10)) written for $k=1(1)n$ leads to a tridiagonal set of n linear equations that can be easily solved for n unknown values of T at the location $(j+1)$.

The two-dimensional heat conduction equation (Eqs. (11) and (12)) is next solved iteratively by the line by line method. Each iteration consists of two alternate sweeps, the first one being in the X-direction and the second in the R-direction. The procedure starts with an assumed temperature distribution over the cylinder and computation is carried out iteratively. The iterations are continued till the temperature distribution over the cylinder obtained in two successive iterations satisfy the convergence criterion of the order of 10^{-5}. Since Eqs. (11) and (12) form a penta-diagonal matrix system, during the X-sweep a set of equations forming tridiagonal matrix system are solved using Thomas algorithm for each fixed j. The terms corresponding to the nodes of $(j+1,k)$ and $(j-1,k)$ are transferred to the right hand side and these are assumed from the previous iteration. Thus Eqs. (11) and (12) can be rewritten during the X-sweep as:

$$T_{j,k-1}\left[-P+\frac{P}{2(k-1)}\right]+T_{j,k}\left[2\beta^2+2P\right]+T_{j,k+1}\left[-P+\frac{P}{2(k-1)}\right]=PQ(\Delta R_1)^2+\beta^2(T_{j-1,k}+T_{j+1,k}), \tag{14}$$

$$T_{j,k}\left[2\beta^2+4P\right]+T_{j,k+1}\left[-4P\right]=PQ\left(\Delta R_1^2\right)+\beta^2\left(T_{j-1,k}+T_{j+1,k}\right), \tag{15}$$

where $\beta=\Delta R_1/\Delta X$. After X-sweep, R-sweep is performed by transferring terms corresponding to $(j,k+1)$ and $(j,k-1)$ for each k. The Eqs. (11) and (12) can be rewritten during R-sweep as:

$$T_{j-1,k}\left[-\beta^2\right]+T_{j,k}\left[2\beta^2+2P\right]+T_{j+1,k}\left[-\beta^2\right]=PQ+P\left[\frac{T_{j,k+1}-T_{j,k-1}}{2(k-1)}\right]+P\left[T_{j,k-1}+T_{j,k+1}\right], \tag{16}$$

$$T_{j-1,k}\left[-\beta^2\right]+T_{j,k}\left[2\beta^2+4P\right]+T_{j+1,k}\left[-\beta^2\right]=PQ+4PT_{j,k+1}. \tag{17}$$

The improved surface temperature distribution of the cylinder resulting from the solution of Eqs. (11) and (12) is again used to solve Eqs. (8)–(10). The overall solution procedure is repeated till the cylinder surface temperature distribution satisfies the convergence criterion of the order of 10^{-3}.

3.3. Computational details

The computer code developed takes care of the fact that the boundary layer thickness has to be increased as we move away from the leading edge. Thus, the hydrodynamic and thermal boundary layer thicknesses are adjusted separately during the computation, while marching in the X-direction. This is done by increasing the number of grids, n, in the R-direction at each X-location. The value of n is chosen so as to ensure that there are at least three grid points where $U\cong 1, T\cong 0$.

For the boundary layer solution, the step size ΔX is increased systematically after marching certain number of steps in the X-direction. This has been done to improve the computational efficiency. The step size close to the leading edge is taken to be very small. This value is almost doubled at an interval of about 10 marching steps. The set of the grid sizes ΔX and the number of steps marched with each ΔX is given in Table 1.

While ΔX can be assigned any value without difficulty, the same is not applicable for the value of ΔR because of the central differencing employed for several terms in the R-direction. Hence it is easier to keep the vale of ΔR uniform. However, due to large gradients of velocity and temperature near the cylinder surface, ΔR must be kept quite small near these regions. Then uniform ΔR across the whole boundary layer thickness, would not only increase the number of simultaneous equations to be solved (which requires excessive computer time for solution), but also involves large round-off error. An alternative is to use a fine mesh size (ΔR) in regions of large gradients and a relatively coarse grid away from it. This requires a modification of the discretized equations at locations where the grid size changes and this was done by introducing a second order algebraic interpolation scheme. An efficient self-adaptive grid scheme proposed by Nakahashi and Deiwart [11] is used along the R-direction. This makes the computer code more efficient apart from yielding more accurate results at the expense of a marginal increase in computational time. The subroutine for adaptation is called at pre-specified X-locations in the marching direction so as to readapt the grid points along the R-direction.

The self-adaptive grid generation technique distributes values of ΔR within the maximum and minimum specified values of ΔR. A minimum ΔR value of 0.02 and a maximum value of 0.1 were chosen. The subroutine for adaptation was called after every 20 steps. For the first 20 steps a uniform ΔR value of 0.04 was chosen.

In order to validate the computer code developed, the flow past a flat plate at zero incidence and constant properties was computed with the present code. The results obtained were compared with the Blasius solution for the flat plate and found to be very close.

Table 1
Step sizes in X direction

Sl. no.	ΔX	No. of steps	X value reached
1.	0.0001	100	0.01
2.	0.001	10	0.02
3.	0.002	10	0.04
4.	0.005	12	0.1
5.	0.01	90	1.0

For the solution of the two-dimensional heat conduction equation, a constant grid size of 0.01 is chosen in both the axial and radial directions. The knowledge of the surface temperatures at grids intermediate to these grids (required during the subsequent solution of the boundary layer equations, where smaller grid sizes are used) is obtained by Lagrangian interpolation.

4. Results and discussion

The computer code developed and tested has been used to analyse the conjugate forced convection–conduction heat transfer in a heat generating vertical cylinder. The results are presented for a range of values of conduction–convection parameter, heat generation parameter and length to diameter ratio keeping the Prandtl number Pr of the flowing fluid constant at 0.005. Special emphasis is given to the effect of these parameters on the radial temperature distribution in the cylinder as well as the boundary layer.

4.1. Axial velocity profiles

The dimensionless axial velocity U profiles at various X-locations on the cylinder are shown in Fig. 2. It is observed that the profile near the leading edge has steeper gradient compared to that away from it. This depicts the growth of the boundary layer in the axial direction. The non-similar nature of the flow is clearly evident from the dependence of these profiles on the value of X. The axial velocity profiles approach the value

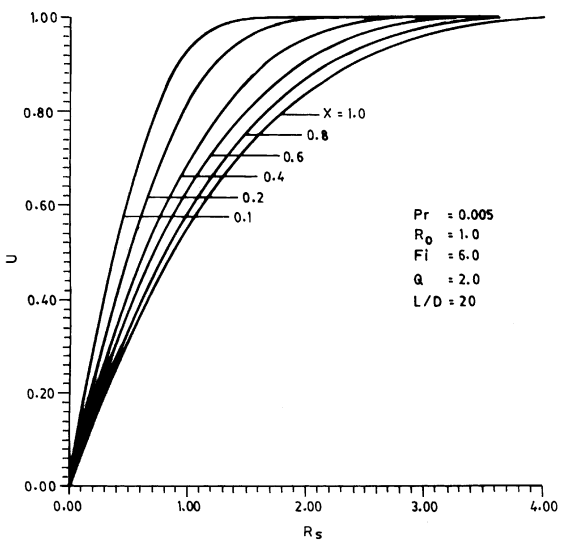

Fig. 2. Longitudinal velocity distribution in the boundary layer on a vertical cylinder at different X-locations.

of that obtained by similarity solution only towards the trailing edge.

4.2. Radial velocity profiles

Fig. 3 shows the dimensionless radial velocity profiles at different axial locations. It is clear that the radial velocity up to some distance from the leading edge, at first increases and then decreases. This is due to the fact that entrainment of the fluid into the boundary layer will be more near the leading edge compared to that far from it. The entrainment of fluid into the boundary layer decreases toward the trailing edge. These profiles also depict the non-similar nature of the flow as explained in previous section.

4.3. Temperature profiles in the boundary layer

Fig. 4 depicts the radial temperature distribution in the boundary layer at various axial locations. On comparison with velocity profiles depicted in Figs. 2 and 3, it is noticed that the growth of the thermal boundary layer is much faster than the velocity boundary layer. This is due to the fact that very low value of Prandtl number corresponding to that for liquid metals is used in the solution. This figure also illustrates the growth of the thermal boundary layer. It can be noticed that the temperature along the surface of the cylinder increases upto a certain distance from leading edge and attains very near to a constant value at $X = 0.1$.

Fig. 5 illustrates the effect of conduction–convection parameter, Fi on the radial temperature distribution in the cylinder at an axial location $X = 0.1$. It is observed

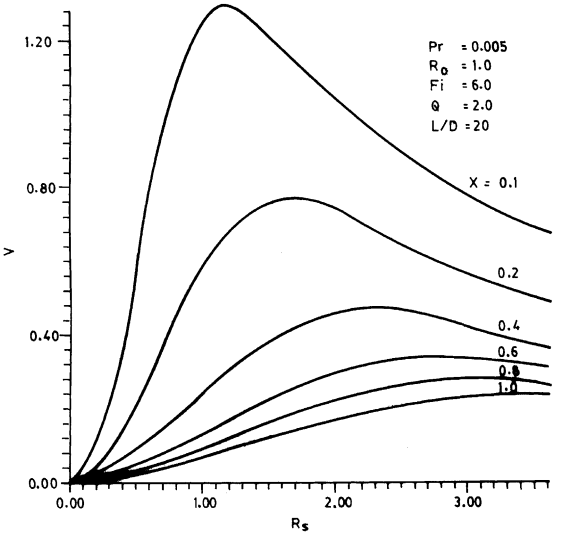

Fig. 3. Transverse velocity distribution in the boundary layer on a vertical cylinder at different X-locations.

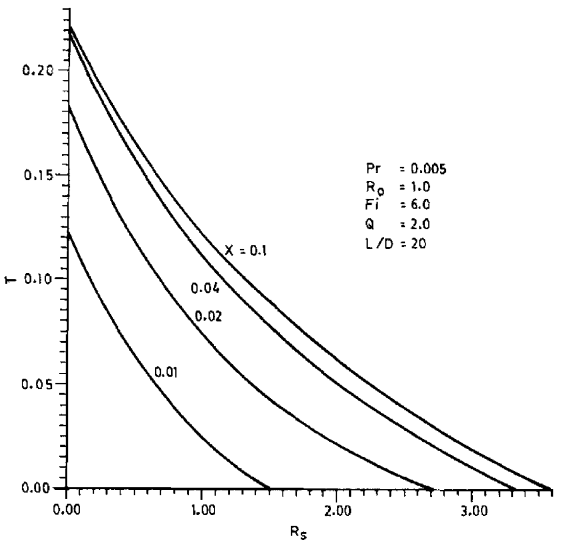

Fig. 4. Temperature distribution in the boundary layer on a vertical cylinder at different X-locations.

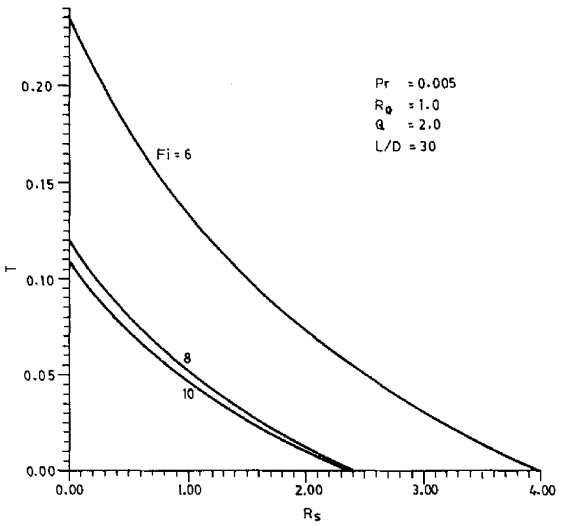

Fig. 5. Effect of conduction–convection parameter on temperature distribution in the boundary layer at $X = 0.1$.

that as Fi increases, the thickness of the thermal boundary layer decreases. This is due to the fact that increase in Fi is mainly due to the thermal conductivity of the flowing fluid. In other words, increase in Fi, results in higher rate of heat dissipation to the fluid, which is most desirable in many engineering applications.

The effect of heat generation parameter, Q on the radial temperature distribution in the boundary layer at $X = 0.1$ is shown in Fig. 6. It is seen that increase in Q increases the thickness of the thermal boundary layer. Even though there is no appreciable change in the

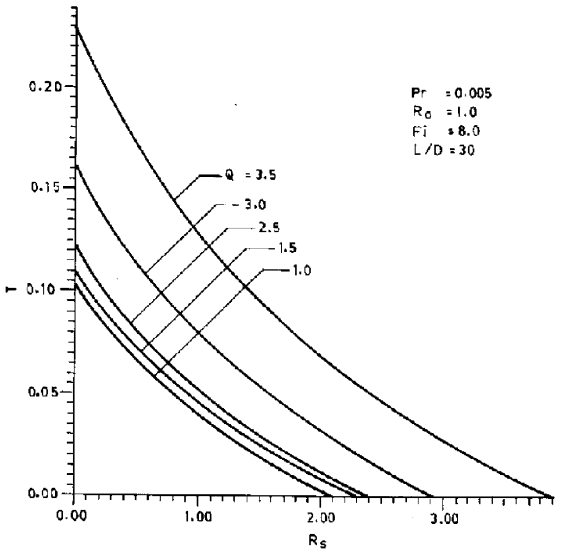

Fig. 6. Effect of heat generation parameter on the temperature distribution in the boundary layer at $X = 0.1$.

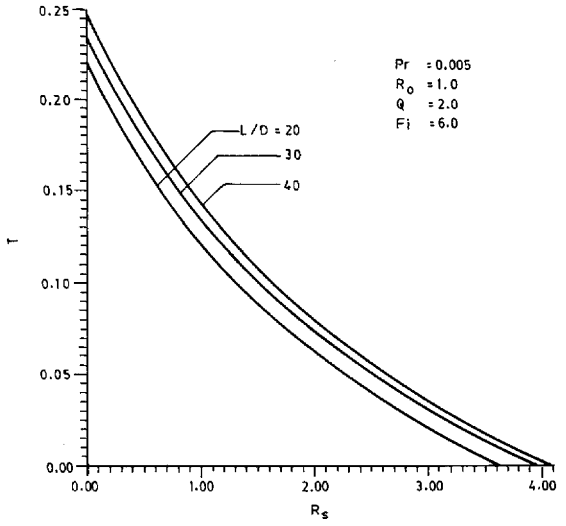

Fig. 7. Effect of L/D ratio on the temperature distribution in the boundary layer at $X = 0.1$.

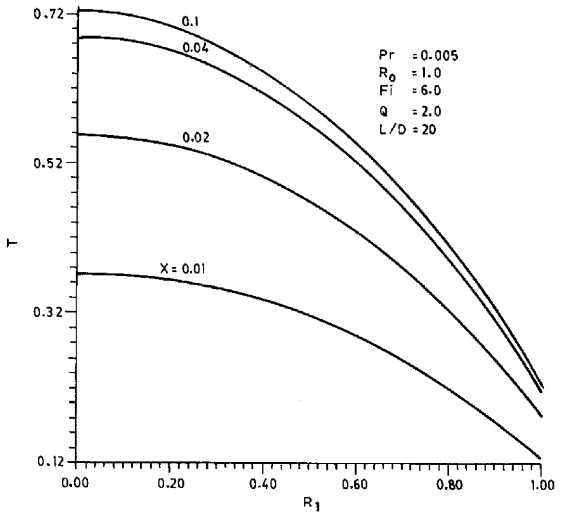

Fig. 8. Radial temperature distribution in the cylinder at different X-locations.

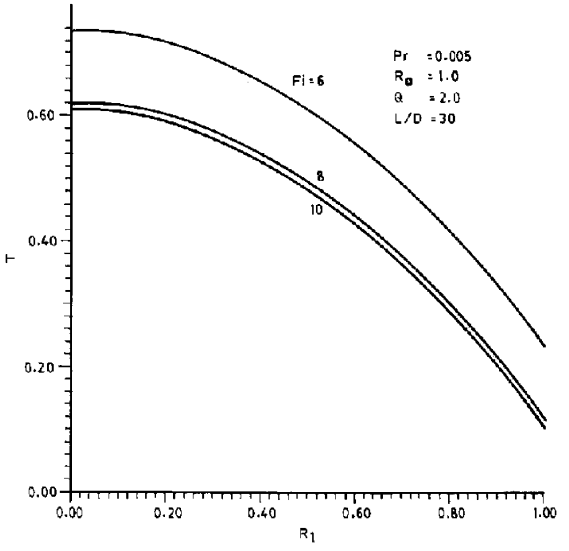

Fig. 9. Effect of conduction–convection parameter on the temperature distribution in the cylinder at $X = 0.1$.

temperature gradient in the boundary layer, overall temperature of the fluid is increased. This may be attributed to the fact that higher value of Fi which is kept constant facilitates dissipation to the flowing fluid. Increase in the surface temperature due to increase in Q is also observed. Based on the above observation it must be noted that there is a limit to which Q can be increased.

Fig. 7 shows the effect of length to diameter ratio L/D of the cylinder on the radial temperature distribution in the boundary layer at $X = 0.1$. It is evident from the figure that the thickness of the boundary layer, the cylinder surface temperature and the fluid temperature are not significantly increased. However, temperature gradient in the fluid remains more or less the same. The above observation is in good agreement of the fact that higher L/D ratio corresponds to higher flow Reynolds number which in turn gives rise to higher convective heat transfer coefficient resulting in higher rate of energy dissipation to the fluid. However,

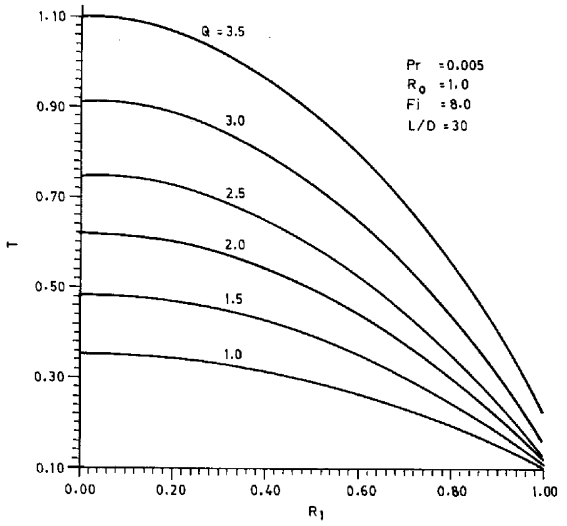

Fig. 10. Effect of heat generation parameter on the temperature distribution in the cylinder at $X = 0.1$.

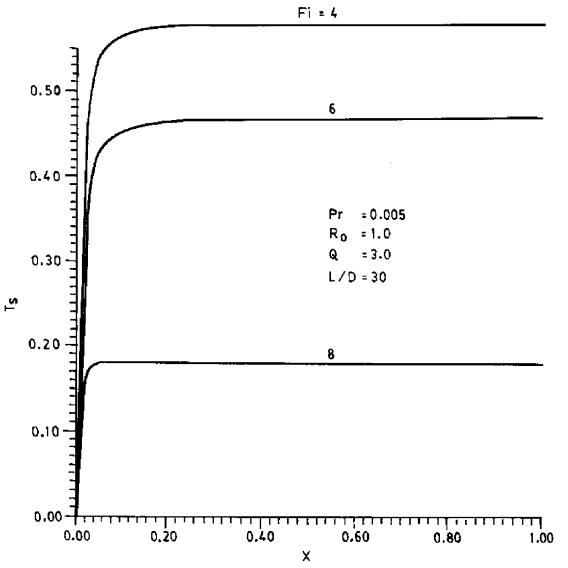

Fig. 12. Effect of conduction–convection parameter on the axial surface temperature distribution.

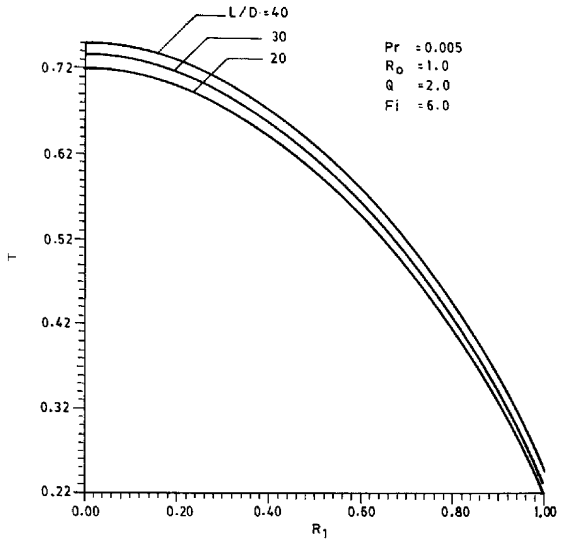

Fig. 11. Effect of L/D ratio on the radial temperature distribution in the cylinder at $X = 0.1$.

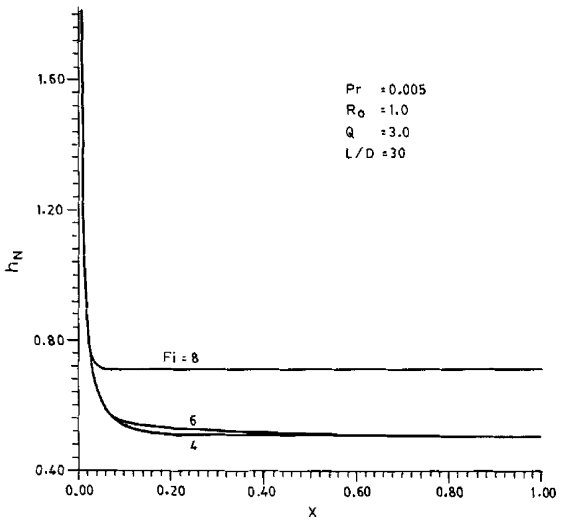

Fig. 13. Effect of conduction–convection parameter on the local heat transfer coefficient.

all the energy dissipated to the fluid in radial direction may not be carried away by the flowing fluid. This may be the reason that there is slight increase in temperature of the fluid.

4.4. Temperature profiles in the cylinder

Fig. 8 presents the radial temperature distribution in the cylinder at four different axial locations. It is noticed that cylinder temperature at the center increases along the axial direction. However, increase in temperature is very much reduced after $X = 0.04$. This trend reveals an important information because temperature in the cylinder must be below certain allowable limit. It is also clear from the figure that radial temperature distribution becomes steeper along the axial direction. This is due to the fact that the rate of heat flux from the surface of the cylinder near the leading edge is more than that away from it. Since the internal heat generation is assumed to be uniform, lesser heat flux from the surface results in

energy storage giving rise to steeper temperature gradient.

The effect of conduction–convection parameter, *Fi* on the radial temperature distribution in the cylinder is shown in Fig. 9. It is seen that increase in *Fi*, results in lower temperature distribution in the cylinder. However, this trend becomes insignificant when *Fi* value is increased from 8 to 10. The maximum temperature at the center of the cylinder has similar trend. The above observed trend can be attributed to the increased energy dissipation to the flowing fluid at higher values of *Fi*. Obviously there will be a limit to which energy dissipation can be increased by increasing the value of *Fi* as internal heat generation is kept constant.

Fig. 10 illustrates the effect of heat generation parameter, Q on the radial temperature distribution in the cylinder at $X = 0.1$. It is quite evident from these figures that increase in Q results in temperature distribution with higher values. The radial temperature gradient is also significantly increased. However, it is interesting to note that the maximum operating temperature in the cylinder limits the extent to which heat generation can be increased. Evidently the above observation is in good agreement of the fact that all the extra energy generated within the cylinder cannot be dissipated keeping *Fi* value constant.

Fig. 11 depicts the effect of length to diameter ratio, L/D on the radial temperature distribution in the cylinder at $X = 0.1$. It is seen that higher values of L/D ratio results is radial temperature distribution with higher values. Even though increase in temperature distribution values are not very significant, increase in L/D ratio will result into higher radial heat flux which is desirable in many application such as the fuel element of a nuclear reactor.

Fig. 12 shows the effect of conduction–convection parameter, *Fi* on the axial surface temperature distribution. It is observed that axial surface temperature increases sharply up to a distance very close to the leading edge and thereafter remains more or less constant. Increase in *Fi* value results in relatively lower value of the surface temperature. In addition the region of variable surface temperature becomes closer to the leading edge. The above observation is due to the fact that higher *Fi* values result in higher energy dissipation to the adjacent fluid resulting in lowering of surface temperature since internal heat generation is kept constant.

4.5. Local heat transfer coefficient

The non-dimensional local heat transfer coefficient is calculated using the relations

$$h_{\mathrm{N}}(X) = h(x)(L/k_{\mathrm{f}})Re^{-1/2} = \frac{-\partial T/\partial R|_{R=R_0}}{T_{\mathrm{s}}(X)}. \qquad (18)$$

The variation of local heat transfer coefficient, h_{N} along the axial direction of the cylinder is shown in Fig. 13. This figure also depicts the effect of conduction–convection parameter, *Fi* on h_{N}. It is evident from Fig. 13 that h_{N} value sharply reduce to a constant value along the axial direction up to a distance very near to the leading edge. Increase in *Fi* values from 4 to 6 results in more or less same distribution of h_{N} along the cylinder. However, increase in *Fi* values from 6 to 8 results in a significant increase in constant value of h_{N} even though up to a certain distance from the leading edge, h_{N} distribution more or less is the same. The effect of variations in *Fi* to a much higher value is felt only after a short distance from the leading edge. However, this distance becomes shorter and shorter for higher values of *Fi*.

5. Conclusions

This paper presents the consideration of radial heat conduction along with internal heat generation in the cylinder in a conjugate heat transfer situation. Although the results obtained have qualitative similarity with previous studies, this numerical work for conjugate heat transfer has demonstrated that consideration of radial heat conduction and internal heat generation presents more significant and realistic results. In particular radial temperature profiles in the boundary layer as well as in the cylinder justify this attempt.

References

[1] A.V. Luikov, V.A. Aleksashenko, A.A. Aleksashenko, Analytical methods of solution of conjugate problems in convective heat transfer, Int. J. Heat Mass Transfer 14 (1971) 1047–1056.
[2] A.V. Luikov, Conjugate convective heat transfer problems, Int. J. Heat Mass Transfer 17 (1974) 257–265.
[3] R. Karvinen, Some new results for conjugated heat transfer in a flat plate, Int. J. Heat Mass Transfer 21 (1978) 1261–1264.
[4] E.M. Sparrow, M.K. Chyu, Conjugate forced convection–conduction analysis of heat transfer in a plate fin, ASME J. Heat Transfer 104 (1982) 204–206.
[5] M.J. Huang, C.K. Chen, Vertical circular pin with conjugated forced convection–conduction flow, J. Heat Transfer 106 (1984) 658–661.
[6] K. Velusamy, V.K. Garg, Heat transfer from a cylindrical fin in combined free-forced flow, Int. J. Heat Fluid Flow 9 (1988) 233–240.
[7] A. Pozzi, M. Lupo, The coupling of conduction with forced convection over a flat plate, Int. J. Heat Mass Transfer 32 (1989) 1207–1214.
[8] W.-S. Yu, H.-T. Lin, T.-Y. Hwang, Conjugate heat transfer of conduction and forced convection along wedges

and a rotating cone, Int. J. Heat Mass Transfer 34 (1991) 2497–2507.

[9] R.W. Hornbeck, Numerical marching techniques in fluid flow with heat transfer, NASA, SP-297, Washington DC, 1973.

[10] P. Roache, Computational Fluid Dynamics, second ed., Hermosa Publishers, Albuquerque, 1982.

[11] K. Nakahashi, G.S. Deiwert, Three dimensional adaptive grid method, AIAA. J. 24 (1986) 948–954.